# Sister trajectories and locality in multiloop string scattering

Steven L. Carbon
*ACTA Inc., 505 N. Orlando Avenue, Mez 3, Cocoa Beach, Florida 32931*
(Received 28 December 1994)

The multiloop corrections to the high-energy behavior of four-tachyon scattering are studied in string theory. In the limit of high center-of-mass energy, $s \to \infty$, for fixed transfer momentum squared, $t$, we obtain the Regge behavior of the first "sister" trajectory in two-loop scattering. The multiloop-generated sisters are found to be independent of propagator twists, which are necessary for exposing tree-level sisters. The presence of these trajectories in higher-order loop diagrams may be sufficient for string theory to be consistent nonperturbatively with locality.

PACS number(s): 11.25.Sq, 11.25.Db, 11.55.Bq

## I. INTRODUCTION

String theory near the Planck scale is not fully understood. There are several characteristics of the current formulation of string field theory (SFT) that suggest strings behave nonlocally in this energy region. If they hold at a fundamental level, then acausality may result, which is probably unacceptable. The most suggestive feature is that strings are extended objects. Second, in well-behaved local field theories, high-energy scattering amplitudes obey the rigorous lower bound set by Cerulus and Martin (CM) [1]. Specifically, in the limit of high center-of-mass energy, $s \to \infty$, for fixed angle $\sin^2(\theta/2) \approx -t/s$ where $t$ is the momentum transfer squared, scattering amplitudes obey $|A(s,t)| \geq e^{-f(\theta)\sqrt{s}\,\ln s}$.

String theory, on the other hand, has the four-point tree-level behavior $|A(s,t)| \to e^{-f(\theta)s}$, which was pointed out even in Veneziano's original paper [2]. Finally, Eliezer and Woodard [3] note that the cubic formulation of string field theory produces an infinite number of Abelian solutions [4]. This causes a breakdown of the initial value problem, since it requires an infinite amount of initial data. They show that attempts to restore this loss of predictability result in acausal behavior, which again leads to nonlocality.

Yet, it has been argued [5] that, since the interaction of strings is local, i.e., at a (mid)point, causality is in fact obeyed. Thus, although strings are extended objects, they are not prevented from exhibiting local behavior. This leaves open the possibility that strings may be obtained from a local field theory. As noted by Thorn [6], it is not necessary that we restrict ourselves to considering only local SFT's, since strings may exist as bound states of a more general local field theory. To lend support to this notion it needs to be shown that string scattering obeys the CM bound, or at a minimum, that it obeys the postulate associated with locality.

The CM bound was derived under the assumptions of the existence of a finite mass gap, polynomial boundedness, and unitarity. Although string theory does not have a finite mass gap, since it has massless particles, it is believed that this probably does not lead to the bound violation. Uniform polynomial boundedness states that, for fixed $t$, the amplitude $|A(s,t)|$ is bounded from above by $s^N$, where $N$ does not depend on $s$ or $t$. There are no elements of the string $S$ matrix that obey this condition in the region $t > N$, since its fixed $t$ behavior goes as $s^t$, i.e., the Regge behavior is linear. Nor does this behavior obey even the weaker condition $N \sim O(|t|^{1/2})$, which Martin showed also yields the CM bound [7]. In quantum field theory, polynomial boundedness is a consequence of locality. As a result, this type of power behavior for $s$ in string theory probably leads to the CM bound violation at each order in perturbation theory. Since each element of the $S$ matrix violates the CM bound, we are left with summing the perturbative series, and thereby obtain unitarity, to determine if the nonperturbative amplitudes obey the bound.

Attempts at restoring the CM bound through unitarity have been made by Gross and Mende [5], and later Mende and Ooguri [8]. These authors examined the dominate elastic scattering behavior at each order in the perturbative expansion. This involves locating the saddle points in moduli space, which were suggested to have the general fixed $t$ scattering behavior

$$A \sim \frac{e^{[\alpha(t)/(g+1)]\ln s}}{(\ln s)^{12g}} , \tag{1}$$

where $g$ is genus number, and the linear Regge trajectory is defined by $\alpha(t) = \alpha' t + \alpha_0$. The "ln$s$" in the denominator in Eq. (1) is indicative of multiple Regge cuts. Unfortunately, due to the form of the energy-dependent coefficients in the exact expressions of the fixed-angle scattering amplitudes, the higher-order quantum corrections could not be controlled during resumming to reach a decisive conclusion. However, Mende and Ooguri were able to show that the CM bound was obeyed for a finite range of energies, which depends on the coupling constant.

Yet, there appears to be no basis for requiring the dominate behavior, at each order in the perturbative expansion, for restoring the CM bound. In the present paper, we investigate a particular subdominate scattering behavior that seems to agree with the lower CM bound limit. The hope is that the resulting perturbative sum will be more yielding to summation. The central feature of our analysis is the so-called "sister" trajectories.

 

Their discovery dates back almost twenty years to Hoyer, Törnqvist, and Webber [9]. These authors showed that in tree-level six-point tachyon scattering the removal of unphysical poles, which threatened the consistency of the theory, required a trajectory with a slope half that of the leading Regge trajectory. Shortly after the discovery of this first sister, Hoyer [10] uncovered the second sister in the eight-point tachyon tree amplitude, and went on to propose the generalization,

$$\alpha_m(t) = \frac{1}{m}\alpha(t) - \frac{1}{2}(m-1) \ , \tag{2}$$

such that the $m$th sister first appears at tree level for $2m + 4$ interacting particles [11,12]. Sisters were subsequently found in the Neveu-Schwarz sector of the Neveu-Schwarz-Ramond (NSR) superstring [13], and related phenomenological implications were discussed [14]. Quirós showed that the first sister also appears in the single-loop six-point diagram, although its identity is absorbed as it renormalizes the corresponding tree-level sister [15]. Finally, several papers have also considered the closed bosonic string and found the same pattern of decoupling in $N$-particle tree scattering as in the open string [16–18].

The first three sister trajectories are shown in Fig. 1 along with the leading Regge trajectory. Due to successively more gradual slopes, the net tendency of the sisters is clearly not linear as $t \to -\infty$. We can find the asymptotic behavior by considering the intersection of two neighboring curves $\alpha_m(t)$ and $\alpha_{m+1}(t)$. Equating these using (2) and then letting $m \to \infty$, we easily find that to lowest order $\alpha(t) \simeq -\frac{1}{2}m^2$. Comparing with (2) gives

$$\alpha_m(t) \simeq -m = -\sqrt{-2\alpha(t)} \approx -\sqrt{-t} \ . \tag{3}$$

Thus, under unitarity, the fixed $t$ scattering behavior now agrees with the weaker polynomial boundedness condition of Martin. To restore the CM bound, for general $N$-particle scattering, we must then exhibit each of the sister trajectories, $\alpha_m(t)$, for all $m$. Since mediating sisters decouple in tree-level exchanges for $m > (N-2)/2$, the approach in this paper will be to demonstrate their existence in multiloop processes. The contributing sisters are those that do not renormalize a lower-order sister. The simplest case to consider is the double-loop diagram

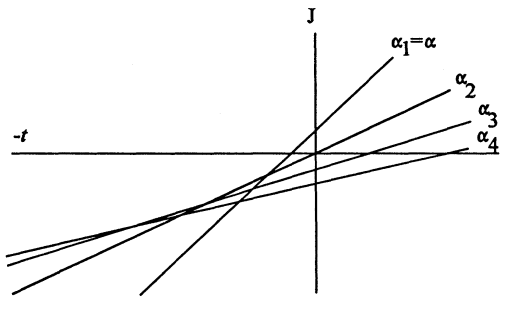


FIG. 1. Plot showing the leading Regge trajectory $\alpha(t)$ and the first three sisters.

of four-point tachyon scattering, where the sister $\alpha_2(t)$ is expected to mediate between two three-point one-loop processes. This topology also allows us to foresee the presence of each of the successive sister trajectories as the number of loops increases. By comparison, there may also be approaches that do not rely on quantum corrections. In Ref. [19], for example, a classical restoration of the CM bound in string theory was suggested through a reinterpretation of the scattering of string states in terms of the sisters as wee partons.

The plan of the paper is as follows. Due to the cumbersome calculations required at the multiloop level, it is desirable to be able to compare our results using two distinct procedures. Thus, here we will introduce an alternate method to the algorithm given in Ref. [19]. In Sec. II, we present a modified approach of the single-Regge high-energy limit for exposing the sister trajectory. The first and second sister trajectories are then obtained in six-point and eight-point tree-level processes, respectively. In Sec. III we will show that the first sister appears in the open string four-point scattering amplitude at the double-loop level. In Sec. IV we give some concluding remarks. Since the sister trajectories appear in the bosonic sector, our results equally apply to the Superstring and Heterotic string. Finally, our notation is as follows. The standard Regge trajectory is given by $\alpha_1 \equiv \alpha(t) = \alpha' t + \alpha_0$, where we choose the open string slope $\alpha' = 1$ and intercept $\alpha_0 = 1$. This leads to a tachyon mass of $m^2 = -1$. The trajectory $\alpha(t_i)$ is associated with the momentum transfer squared $t_i$ across the propagator $z_i$. Finally, the trajectory $\alpha(s_{ij})$ is defined with respect to the energy

$$s_{ij} \equiv -(p_i + p_{i+1} + \ldots + p_j)^2 \ .$$

## II. SINGLE-REGGE LIMIT METHOD

Three different high-energy limit schemes have been employed in the past to uncover the sister trajectories in tree-level scattering processes. The most general is the single-Regge limit where the energy across only one off-shell mediating propagator is allowed to grow large, while across the others it remains relatively small. Even though this is the most desirable limit to apply, since it is the most general, it has until now only been applied to six-point scattering [20]. In their first paper, Hoyer, Törnqvist, and Webber exposed the sister trajectory $\alpha_2(t)$ using the helicity-pole limit [9]. This limit was also used to first exhibit the $\alpha_3(t)$ sister in eight-point scattering [10]. Subsequently, the full spectrum of sisters was found using the even less general multiple-Regge limit [11,12]. Since it is important to display the general nature of the sister trajectories, in this paper we use the single-Regge limit procedure.

The single-Regge limit, in which the transfer momentum squared $t$ is kept fixed, relates to the CM theorem differently than using the fixed-angle limit as employed, for example, by Gross and Mende. The fixed-angle limit allows direct verification that scattering amplitudes obey

the lower CM lower bound. On the other hand, using the single-Regge limit, we are attempting to show that scattering amplitudes obey the weaker fixed $t$ upper bound condition of Martin [7]. Recall that this condition is just one of the three assumptions in the proof of the CM bound but is a direct consequence of locality, which is our main focus. Proving this condition through unitarity will still not be enough, however, to conclude that the CM bound holds in string theory. The finite mass gap will always exist, since eliminating photons or gravitons from string theory are beyond consideration.

Our main goal is to apply the single-Regge limit to a multiloop string scattering process. For this, we must reconsider two features of past approaches, which were necessary for sister trajectories to exist in a tree-level process. First, a four-dimensional space-time was assumed. Though string theories are simplest in critical space-time dimensions of 10 and 26, this restriction can be met in the high-energy limit by allowing momentum to grow large in only four dimensions. Removing this condition would simply mean that we may have to start the search for sisters at a higher $N$-point function, with an appropriate dimensionality constraint. Second, to reach the sections of moduli space, where sister trajectories dominate, requires that at least one off-shell mediating propagator be twisted. Since the original single-Regge limit procedure given in Appendix B of Ref. [20] requires *a priori* knowledge of twists, we modify that approach to eliminate the need for their explicit presence in the initial expression of the amplitude. We detail our method using the six-point function and easily reproduce the result of the above work. For higher point functions, our approach allows many cases to be considered simultaneously, which significantly reduces the necessary effort. Below, we evaluate the eight-point scattering process to highlight this advantage.

### A. Six-particle tree scattering

Figure 2 shows the lowest-order scattering process that exhibits the first sister trajectory, $\alpha_2(t)$. The original observation of Hoyer, Törnqvist, and Webber [9] that suggested there must be other trajectories than the standard Regge trajectory $\alpha(t)$ is as follows. In the limit $s \to \infty$, the six-point amplitude factorizes:

$$A_6 \simeq \Delta(\alpha(t_a))V(\alpha(t_a),\alpha(t_b))\Delta(\alpha(t_b)) \times V(\alpha(t_b),\alpha(t_c))\Delta(\alpha(t_c)) \ . \tag{4}$$

The propagators $\Delta(\alpha)$ have zeros for $\alpha = -1,-2,\ldots$.

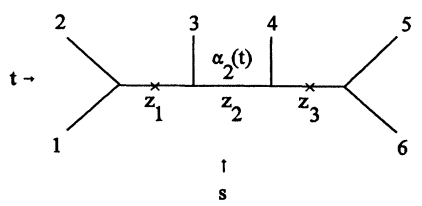


FIG. 2. The first sister $\alpha_2(t)$, requiring twists on both $z_1$ and $z_3$.

On the other hand, the vertices $V(\alpha(t_a),\alpha(t_b))$ have unphysical poles for $\alpha(t_a),\alpha(t_b) = -1,-2,\ldots$, which have the undesirable properties of negative spin ("nonsense") and wrong signature. Now, for $\alpha(t_b)$ there is only one zero coming from the central propagator, while there are two poles coming from the adjacent vertices. This leaves an unphysical pole, which does not appear in the exact expression for the scattering amplitude. For the theory to be consistent there must be some mechanism to cancel this unwanted pole.

To examine the high-energy behavior of scattering amplitudes in a way that makes sense requires that the energy first be analytically continued into the complex plane, e.g., $s \to i\infty$ [21]. With large energy in only four dimensions, there are eight kinematic degrees of freedom, yet nine free parameters. Thus, one must apply a four-dimensionality constraint [22]. Hoyer, Törnqvist, and Webber observed that previous analyses have imposed the dimensionality condition only after the energy had been analytically continued back to the physical plane. The effect of not maintaining the constraint throughout the calculation is that some critical point remains hidden. Imposing the constraint before the back continuation, allows a factorization to occur in the amplitude, which then exposes the critical point. Integration about this point leads to the behavior $|A(s,t)| \to s^{\alpha_2(t)}$ with poles at $\alpha_2(t) = -1,0,1,\ldots$. For $\alpha(t) = -1$, the pole due to the sister trajectory $\alpha_2(t)$ precisely cancels the remaining unphysical pole appearing on the $\alpha(t)$ trajectory.

The sister trajectory $\alpha_2(t)$ is exposed in the high-energy limit of the six-point function only if twists are placed on both of the adjoining propagators as shown in Fig. 2. We begin, however, with the corresponding untwisted amplitude. This is easily calculated in the Fubini-Veneziano formalism from

$$A_6 = \langle 0,p_1|V(p_2)\Delta V(p_3)\Delta V(p_4)\Delta V(p_5)|0,p_6\rangle \ . \tag{5}$$

In general, passing the vertex operators through each other produces factors of the form

$$\exp\left[-2p_i\cdot p_j\sum_{n=1}^{\infty}\frac{z^n}{n}\right] \equiv (1-z)^{2p_i\cdot p_j} \ , \tag{6}$$

where $z$ is the product of coordinates $z_i$, which are associated with the mediating propagators connecting the vertices. Final expressions for the amplitude are usually written in terms of the right-hand factors. The left-hand form is more convenient, however, for locating critical points in the high-energy limit $s \to i\infty$. Consequently, we use the left-hand side of (6) if one of the connecting propagators sees the energy $s$, and the right-hand side for nonoverlapping quantities. In the particular case of Fig. 2, the complete exponential factor is easily found to be

$$\exp\left(2\sum_{n=1}^{\infty}\frac{z_2^n}{n}(-p_2z_1^n-p_3)\cdot(p_4+p_5z_3^n)\right) \ . \tag{7}$$

Substituting the momentum scalar products, the full amplitude becomes

$$A_6 \simeq \int_0^1 dz_1 dz_2 dz_3 z_1^{-1-\alpha(t_1)} z_2^{-1-\alpha(t_2)} z_3^{-1-\alpha(t_3)} (1-z_1)^{-1-\alpha(s_{23})} (1-z_3)^{-1-\alpha(s_{45})} \times \exp\left( \sum_{n=1}^{\infty} \frac{z_2^n}{n} [z_1^n (s_{24} - s_{34}) + z_1^n z_3^n \tilde{s} + s_{34} + z_3^n (s_{35} - s_{34})] \right) , \tag{8}$$

where

$$\tilde{s} = s_{34} + s_{61} - s_{24} - s_{35} . \tag{9}$$

In writing (8), we have also dropped terms in the exponential, which can be safely neglected in the high-energy limit.

We are now in a position to impose the four-dimensionality constraint, which, in the high-energy limit, is given by [22]

$$\frac{s_{35} s_{24}}{s_{34} s_{61}} = 1 . \tag{10}$$

Applying this constraint to (8) allows the argument of the exponential to be factorized, giving

$$A_6 \simeq \int_0^1 dz_1 dz_2 dz_3 z_1^{-1-\alpha(t_1)} z_2^{-1-\alpha(t_2)} z_3^{-1-\alpha(t_3)} (1-z_1)^{-1-\alpha(s_{23})} \times (1-z_3)^{-1-\alpha(s_{45})} \exp\left( \tilde{s} \sum_{n=1}^{\infty} \frac{z_2^n}{n} (z_1^n - x_1)(z_3^n - x_3) \right) , \tag{11}$$

where

$$x_1 = \left(1 - \frac{s_{61}}{s_{35}}\right)^{-1} , \quad x_3 = \left(1 - \frac{s_{61}}{s_{24}}\right)^{-1} . \tag{12}$$

To evaluate the high-energy limit, we let $\tilde{s} \to i\infty$, where the real part of $\tilde{s}$ is held fixed in the strip of convergence. The result is a Fourier integral whose asymptotic behavior is dominated by its critical points [21]. For $(x_1, x_3)$ to be a useful critical point it must fall within the integration region, $0 < z_1, z_3 < 1$. Critical points taken at the boundaries do not produce sisters. Since the boundary of the integration region is not included, the factors in (11), other than the exponential, can be ignored during integration. To recover the proper limit $\tilde{s} \to i\infty$, we obtain a double critical point by choosing the phases

$$\begin{aligned} &s_{34}, s_{61} \to i\infty , \\ &s_{24}, s_{35} \to -i\infty . \end{aligned} \tag{13}$$

This is completely equivalent to twisting the propagators corresponding to $z_1$ and $z_3$, since energies that overlap an odd number of twisted propagators change sign. In other words, the role of the twists here is to place the critical point inside the integration region.

The leading trajectory of the first sister from (11) is obtained by integrating about the $n = 1$ critical point, i.e.,

$$|z_1 - x_1| \le \epsilon , \quad |z_3 - x_3| \le \epsilon , \tag{14}$$

where the relative smallness of $\epsilon$ with respect to $\tilde{s}^{-1}$ will be determined shortly. Choosing higher-order critical points would lead to the daughter trajectories associated with the first sister. For the leading-order critical point evaluation of (11), we need retain only up to the $n = 2$ term in the exponential. After shifting $z_1$ and $z_3$, we obtain

$$A_6 \sim x_1^{-1-\alpha(t_1)} x_3^{-1-\alpha(t_3)} (1-x_1)^{-1-\alpha(s_{23})} \times (1-x_3)^{-1-\alpha(s_{45})} I_6 , \tag{15}$$

where the integral is given by

$$I_6 = \int_0^1 dz_2 z_2^{-1-\alpha(t_2)} e^{\tilde{s} z_2^2 c} \int_{-\epsilon}^{\epsilon} dz_1 dz_3 \exp[\tilde{s} z_2 z_1 z_3] , \tag{16}$$

and we have defined the constant

$$c = \tfrac{1}{2} x_1 x_3 (x_1 - 1)(x_3 - 1) . \tag{17}$$

Setting $y = -i\epsilon z_2 z_3 \tilde{s}$, yields

$$I_6 = i(\epsilon\tilde{s})^{-1} \int_0^1 dz_2 z_2^{-2-\alpha(t_2)} e^{\tilde{s} z_2^2 c} \times \int_{-\epsilon}^{\epsilon} dz_1 \int_{-y_0}^{y_0} dy \exp(i\epsilon^{-1} y z_1) , \tag{18}$$

where $y_0 = -i\epsilon^2 z_2 \tilde{s}$. Integrating over $z_1$ we easily find

$$I_6 = \tilde{s}^{-1} \int_0^1 dz_2 z_2^{-2-\alpha(t_2)} e^{\tilde{s} z_2^2 c} \times \int_{-y_0}^{y_0} dy \frac{\exp(iy) - \exp(-iy)}{y} , \tag{19}$$

where the resulting $y$ integral is now symmetric. If $z_3$ were not critical, taking the limit $\epsilon \to 0$ here would give $I_6 = 0$ (use $dy \sim \epsilon$). This explains the need for a double critical point, which is not present in either the four- or five-point amplitudes. Now, in the high-energy limit $\tilde{s} \to i\infty$, $y_0 \to \infty$, and so the integration over $y$ gives $2i\pi$.

To obtain a convergent representation for the $z_2$ integral, we now take $\tilde{s} \to -\infty$, after which we will analytically continue back to $\tilde{s} \to \infty$. Define $z = -\tilde{s}z_2^2 c$, which gives

$$I_6 = i\pi(-\tilde{s}c)^{(1/2)\alpha(t_2)+(1/2)}\tilde{s}^{-1} \times \int_0^\infty dz\, z^{-(3/2)-(1/2)\alpha(t_2)}e^{-z} . \quad (20)$$

Note, that for us to consistently write $z = -y^2\epsilon^{-4}\tilde{s}^{-1}c$ we must have $\epsilon > \tilde{s}^{-1/4}$ to reach the lower limit $z \to 0$ for fixed $y$. Doing the $z$ integral gives $\Gamma[-\frac{1}{2} - \frac{1}{2}\alpha(t_2)]$, which is valid only for $\alpha(t_2) < -1$. In this region the first sister trajectory dominates the $\alpha(t)$ trajectory. Collecting everything together, the complete amplitude is then

$$A_6 \sim i\pi(-\tilde{s}c)^{(1/2)+(1/2)\alpha(t_2)}\tilde{s}^{-1} \times\Gamma[-\tfrac{1}{2} - \tfrac{1}{2}\alpha(t_2)]x_1^{-1-\alpha(t_1)}x_3^{-1-\alpha(t_3)} \times(1-x_1)^{-1-\alpha(s_{23})}(1-x_3)^{-1-\alpha(s_{45})} . \quad (21)$$

We now analytically continue the energy back by making the replacement $-\tilde{s} \to e^{-i\pi}\tilde{s}$. Using $\alpha_2(t_2) = \frac{1}{2}\alpha(t_2) - \frac{1}{2}$, which corresponds to the first sister trajectory, and simplifying, we finally arrive at

$$A_6 \sim -i\pi e^{-i\pi\alpha_2(t_2)}2^{-\alpha_2(t_2)-1}\tilde{s}^{\alpha_2(t_2)} \times\Gamma[-\alpha_2(t_2) - 1]x_1^{\alpha_2(t_2)-\alpha(t_1)}x_3^{\alpha_2(t_2)-\alpha(t_3)} \times(1-x_1)^{\alpha_2(t_2)-\alpha(s_{23})}(1-x_3)^{\alpha_2(t_2)-\alpha(s_{45})} . \quad (22)$$

Since each energy in $\tilde{s}$ overlaps with $s_{34}$, the Regge behavior $\tilde{s}^{\alpha_2(t_2)}$ shows that the central propagator in Fig. 2 sees the sister. Using the four-dimensionality constraint (10) we can write

$$\tilde{s} = s_{34} + s_{61} - s_{24} - s_{35} = s_{61}^{-1}(s_{35} - s_{61})(s_{24} - s_{61}) , \quad (23)$$

and easily recover Eq. B.19 of Ref. [20].

Examining the $\Gamma$ function in (22), we see that the poles of the first sister trajectory are at $\alpha_2(t_2) = -1, 0, 1, \ldots$. Our approach makes it particularly easy to determine the signature $\tau$ of these poles. Twisting the sister propagator $z_2$ changes the sign of each of the overlapping energies. Although both the numerator and denominator of $x_1$ and $x_3$ change sign in Eq. (12), the signs of the energy ratios remain unchanged. Thus, the twisted and untwisted diagrams can be added together giving an overall weight factor $\tau + 1$. Therefore, the poles of $\alpha_2(t_2)$ have pure positive signature. Since these poles correspond to odd values of spin, i.e., $\alpha(t_2) = 1, 1, 3, \ldots$, they have an unphysical wrong signature.

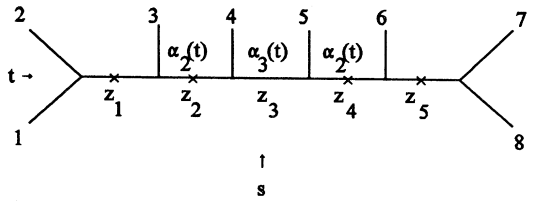


FIG. 3. At tree level, the second sister $\alpha_3(t)$ first appearing in eight-point scattering. Concurrently, $z_2$ and $z_4$ see $\alpha_2(t)$.

To summarize, for the existence of the first sister it was necessary that the argument of the exponential factorize, producing a 2-tuple critical point. Integrating over both coordinates, in effect, removed the linear power of the propagator variable $z_2$ from the exponential. In general, integrals of the form

$$I = \int_0^1 z^{-\alpha-1-n}\exp(-cz^m) \quad (24)$$

in the limit $c \to \infty$ integrate to

$$I \simeq \frac{1}{m}\Gamma\left(-\frac{\alpha}{m} - \frac{n}{m}\right)c^{(\alpha/m)+(n/m)} \quad \text{for } \alpha < -n . \quad (25)$$

Thus, sisters do not appear in either four- or five-point scattering, since both retain the linear power of $z$. Furthermore, to produce the second sister $\alpha_3(t)$, both the linear and quadratic powers of $z$ must be integrated away, leaving the cubic power. This occurs when the critical point is a 4-tuple, which first arises in the eight-point scattering amplitude.

### B. Eight-particle tree scattering

In this section we will expose the second sister, $\alpha_3(t)$, in the open string tree diagram of Fig. 3, where the sister appears across the propagator associated with $z_3$ [12]. In the corresponding amplitude, we isolate the relevant terms by including in the exponential only quantities that overlap the central propagator. We gather the other terms into a function $f(z_1, z_2, z_4, z_5)$, whose exact form can be ignored, since, as shown in the last section, the sisters depend only on the exponential factor. The evaluation of the eight-point diagram has, until now, only been carried out under the multiple-limit methods [10,12], and never using the more general single-Regge limit taken here.

From Fig. 3, ignoring twists, we immediately write down

$$A_8 = \int_0^1 \prod_{i=1}^5 dz_i f(z_1, z_2, z_4, z_5) z_3^{-1-\alpha(t_3)} \exp\left[2\sum_{n=1}^\infty \frac{z_3^n}{n}(-p_2 z_1^n z_2^n - p_3 z_2^n - p_4)\cdot(p_5 + p_6 z_4^n + p_7 z_4^n z_5^n)\right] . \quad (26)$$

Substituting in the high-energy limit values of the momentum scalar products gives the eight-tachyon amplitude

$$A_8 \simeq \int_0^1 \prod_{i=1}^{5} dz_i f(z_1,z_2,z_4,z_5) z_3^{-1-\alpha(t_3)} \exp\left( \sum_{n=1}^{\infty} \frac{z_3^n}{n} [z_1^n z_2^n (s_{25}-s_{35}) + z_1^n z_2^n z_4^n (s_{26}-s_{25}+s_{35}-s_{36}) \right.$$
$$+ s_{45} + z_1^n z_2^n z_4^n z_5^n \tilde{s} + z_2^n (s_{35}-s_{45}) + z_4^n (s_{46}-s_{45})$$
$$\left. + z_4^n z_5^n (s_{47}-s_{46}) + z_2^n z_4^n (s_{36}-s_{35}+s_{45}-s_{46}) + z_2^n z_4^n z_5^n (s_{37}-s_{36}+s_{46}-s_{47})] \right) , \tag{27}$$

where, now,

$$\tilde{s} = (s_{81} - s_{26} + s_{36} - s_{37}) . \tag{28}$$

As before, each energy in $\tilde{s}$ overlaps with the energy $s_{34}$ associated with the proposed sister propagator.

Applying the high-energy four-dimensionality constraints

$$\frac{s_{81}s_{36}}{s_{26}s_{37}} = 1 , \quad \frac{s_{81}s_{35}}{s_{25}s_{37}} = 1 , \quad \frac{s_{81}s_{46}}{s_{26}s_{47}} = 1 , \quad \frac{s_{81}s_{45}}{s_{25}s_{47}} = 1 , \tag{29}$$

factorizes the argument of the exponential yielding

$$A_8 \simeq \int_0^1 \prod_{i=1}^{5} dz_i f(z_1,z_2,z_4,z_5) z_3^{-1-\alpha(t_3)} \exp\left[ \tilde{s} \sum_{n=1}^{\infty} \frac{z_3^n}{n} (z_1^n - x_1)(z_2^n - x_2)(z_4^n - x_4)(z_5^n - x_5) \right] , \tag{30}$$

where

$$x_1 = \frac{s_{36}-s_{37}+s_{47}-s_{46}}{\tilde{s}} , \quad x_4 = \frac{s_{25}-s_{35}}{s_{26}-s_{25}+s_{35}-s_{36}} ,$$
$$x_2 = \frac{s_{47}-s_{46}}{s_{37}-s_{36}+s_{46}-s_{47}} , \quad x_5 = \frac{s_{25}-s_{26}+s_{36}-s_{35}}{\tilde{s}} . \tag{31}$$

For the critical point $(x_1, x_2, x_4, x_5)$ to be inside the integration region, we must place twist on each of the associated propagators and apply an additional four-dimensionality constraint:

$$\frac{s_{36}s_{45}}{s_{35}s_{46}} = 1 . \tag{32}$$

Consequently, due to the twists we have the sign changes

$$s_{26}, s_{35}, s_{37}, s_{46} \to -i\infty . \tag{33}$$

To remove the first two powers of $z_3$ in the exponential in (30), and to obtain a leading trajectory, we will integrate around

$$|z_1 - x_1| \le \epsilon , \quad |z_2 - x_2| \le \epsilon ,$$
$$|z_4 - \sqrt{x_4}| \le \epsilon , \quad |z_5 - \sqrt{x_5}| \le \epsilon . \tag{34}$$

Clearly, this is just one of many critical points that we could have chosen. By writing $z_4^2 - x_4 = (z_4 - \sqrt{x_4})(z_4 + \sqrt{x_4}) \sim 2\sqrt{x_4}(z_4 - \sqrt{x_4})$, etc., and shifting the $z$'s, we find

$$A_8 \sim f(x_1, x_2, \sqrt{x_4}, \sqrt{x_5}) \int_0^1 dz_3 z_3^{-1-\alpha(t_3)} e^{\tilde{s} z_3^3 c} \int_{-\epsilon}^{\epsilon} dz_1 \int_{-\epsilon}^{\epsilon} dz_2 \exp[z_3 z_1 z_2 \tilde{s} (\sqrt{x_4} - x_4)(\sqrt{x_5} - x_5)]$$
$$\times \int_{-\epsilon}^{\epsilon} dz_4 \int_{-\epsilon}^{\epsilon} dz_5 \exp[2 z_3^2 z_4 z_5 \tilde{s} \sqrt{x_4 x_5} (x_1^2 - x_1)(x_2^2 - x_2)] , \tag{35}$$

where

$$c = \tfrac{1}{3}(x_1^3 - x_1)(x_2^3 - x_2)(x_4^{3/2} - x_4)(x_5^{3/2} - x_5) . \tag{36}$$

The last four integrals in (35) can be done in pairs, resulting in

$$A_8 \sim -4\pi^2[2\tilde{s}^2 x_4 x_5(x_1^2-x_1)(x_2^2-x_2)(1-\sqrt{x_4})(1-\sqrt{x_5})]^{-1} f(x_1,x_2,\sqrt{x_4},\sqrt{x_5}) \int_0^1 dz_3 z_3^{-4-\alpha(t_3)} e^{\tilde{s}z_3^3 c} \ . \quad (37)$$

Using (25) and taking the limit $\tilde{s} \to -\infty$, then gives

$$A_8 \sim -\tfrac{2}{3} f(x_1,x_2,\sqrt{x_4},\sqrt{x_5})\pi^2(-\tilde{s}c)^{(1/3)\alpha(t_3)+1}\Gamma[-\tfrac{1}{3}\alpha(t_3)-1] \times[\tilde{s}^2 x_4 x_5(x_1^2-x_1)(x_2^2-x_2)(1-\sqrt{x_4})(1-\sqrt{x_5})]^{-1} \ , \quad (38)$$

which is valid only for $\alpha(t_3) < -3$. Again, we analytically continue back by replacing $-\tilde{s}$ with $e^{-i\pi}\tilde{s}$. Thus, we find the Regge behavior $A_8 \propto \tilde{s}^{(1/3)\alpha(t_3)-1} \equiv \tilde{s}^{\alpha_3(t_3)}$, which corresponds to the second sister trajectory. The first pole at $\alpha_3(t_3) = -2$ cancels the pole of the first sister trajectory at $\alpha_2(t_3) = -2$. The daughters of $\alpha_3(t_3)$ cancel the other poles at $\alpha_2(t_3) = -3, -4, \ldots$.

When the central propagator in Fig. 3 mediates the second sister $\alpha_3(t)$, the adjacent propagators $z_2$ and $z_4$ see the first sister $\alpha_2(t)$. The corresponding amplitudes can easily be computed by writing the exponential factor in (26) in terms of the appropriate overlap quantities, taking the corresponding high-energy limit, and then integrating over a 2-tuple. However, if the intent is just to prove the existence of these sisters, then the form of Eq. (30) suffices. By observation, this expression also indicates that the $\alpha_2(t_3)$ trajectory occurs on the central propagator if there are either two or three twisted propagators, with at least one on both sides. In previous methods, exposing each of these sisters required considering separate cases by including the various twists in the initial amplitude. Consequently, we now have a more direct procedure for examining sisters in loop diagrams, where it is not clear what role twists will play.

## III. DOUBLE-LOOP FOUR-TACHYON SCATTERING

We turn now to four-point scattering, which at tree level is known not to exhibit any sister behavior. The single-loop diagram does not have a sister either, since its scattering amplitude has at most a single critical point. Thus, the first sister trajectory is expected to require at least two loops. Since the single-Regge procedure uncovers the dominate scattering behavior in selected parts of moduli space, we must be careful to avoid processes where the sisters have to compete with Regge cuts. For example, Fig. 4 displays the two lowest order diagrams

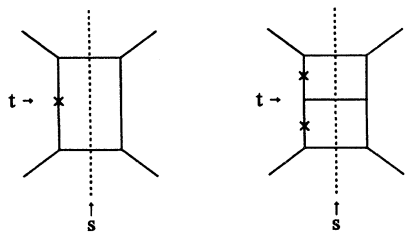


(a) (b)

FIG. 4. The Regge cut behavior across the dotted line.

with the cuts. The general form of an amplitude dominated by a cut is given by

$$A \sim \frac{e^{[\alpha(t)/(g+1)]\ln s}}{(\ln s)^p} \ , \quad (39)$$

for some constant $p$. This shows that for the double-loop process the cut has the same Regge slope as the second sister. As $t$ goes to negative infinity, the high-energy amplitude with the cut will eventually dominate the amplitude of any potential sister trajectory $\alpha_2(t)$. In general, the $n$th cut occurs at one lower order process than that of the $n$th sister, but with a trajectory above the sister in the high-energy limit.

This leads us to focus on processes in which the sister appears outside the loop. Two such topologies are shown in Fig. 5. Although cuts may still arise if twists are required in either loop, the procedure given in the last section allows us to isolate terms in the scattering amplitude that emphasize only the candidate propagator. We will evaluate the limiting situation where the loops are sufficiently separated such that they and the connecting propagator can be treated as individual objects. Both amplitudes may be constructed by sewing together two single-loop diagrams. For this, we use the formalism from Appendix D of Di Vecchia *et al.* [23], where the open string $N$-point multiple-loop vertex has the form

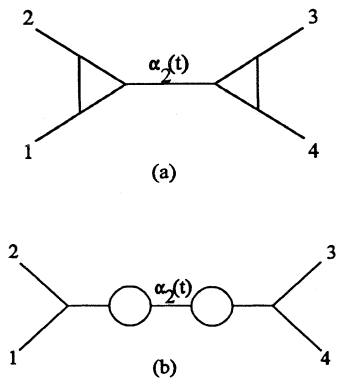


FIG. 5. Two distinct topologies for producing the $\alpha_2(t)$ sister in double-loop four-point scattering.

$$V_{(N;g)} \propto \int d^D\tilde{p}\, \exp[i\pi\tilde{p}\cdot\tau\cdot\tilde{p}+\tilde{p}\cdot B+C]\ , \qquad (40)$$

and where $\tau$ is the period matrix. Completing the square and integrating over the loop momentum $\tilde{p}$ gives

$$V_{(N;g)} \propto \frac{1}{(\det i\pi\tau)^{D/2}}\exp[-i\pi B\cdot\tau^{-1}\cdot B+C]\ . \qquad (41)$$

The factorized four-tachyon double-loop amplitude is then given by

$$A_{(4;2)} = \int_0^1 dz \prod_{i=1}^{4} dz_i \int d\mu \langle 0,p_1,p_2| \exp\left[-\frac{1}{2}\frac{B_L^2}{\ln k_1}+C_L\right] z^{L_0^{(c)}-2} \exp\left[-\frac{1}{2}\frac{(B_R^\dagger)^2}{\ln k_2}+C_R^\dagger\right] |0,p_3,p_4\rangle\ , \qquad (42)$$

where the subscripts $L$ and $R$ refer to the left and right loop, respectively, and the superscript on $L_0^{(c)}$ labels the leg connecting the loops. The period matrix has been reduced to the single-loop case $\tau = 2\pi i \ln k$, where $k$ will be defined below. The details of the measure $d\mu$, which is a function of $k_1$ and $k_2$, may be suppressed in the analysis below as long as the boundaries of the integration region are avoided.

In the multiple-loop case, the coefficient $B_\mu$ in (40) is given by (with $\alpha' = 1$)

$$B_\mu = \sqrt{2}\sum_{i=1}^{3}\sum_{m=0}^{\infty}\frac{\alpha_m^{(i)}}{m!}\partial_z^m \times \left({}^{(\mu)}\sum_{\alpha}\ln\frac{\xi_\mu - T_\alpha(V_i(z))}{\eta_\mu - T_\alpha(V_i(z))}\frac{\eta_\mu - T_\alpha(z_0)}{\xi_\mu - T_\alpha(z_0)}\right)_{z=0}\ , \qquad (43)$$

where $z_0$, $\eta_\mu$, and $\xi_\mu$ are fixed points, and a product of Schottky group elements is defined by

$$T_\alpha = S_{\mu_1}^{n_1}S_{\mu_2}^{n_2}\cdots S_{\mu_r}^{n_r}\ ,\quad r=1,2,\ldots,g\ , \qquad n_i\in Z/\{0\}\ ;\quad \mu_i\neq\mu_{i+1}\ , \qquad (44)$$

where $g$ is the genus number. Also, ${}^{(\mu)}\sum_\alpha$ means that the sum is over all elements of the Schottky group except that the leftmost element in $T_\alpha$ cannot be $S_\mu^n$. It would be quite difficult to proceed from this point if it were not for the fact that we have factorized into single loops. In practice, the Schottky group formalism describing the multiple-loop diagrams is much too formal to be of use. In the single-loop case $T_\alpha = S_1^n$ and $S_1^n(y) = k^n y$, where $k$ is the multiplier and related to the radius of the loop. Here, however, the sum restriction leaves just the identity. Finally, for one loop $\xi\to\infty, \eta_1\to 0$. Thus, dropping the loop index,

$$B = \sqrt{2}\sum_{i=1}^{3}\sum_{m=0}^{\infty}\frac{\alpha_m^{(i)}}{m!}\left(\partial_z^m \ln\frac{z_0}{V_i(z)}\right)_{z=0}\ , \qquad (45)$$

where the projective transformation is explicitly given by

$$V_i(z) = \frac{z_{i-1}(z_i-z_{i+1})z + z_i(z_{i+1}-z_{i-1})}{(z_i-z_{i+1})z+(z_{i+1}-z_{i-1})} \equiv \frac{a_1 z+a_2}{a_3 z+a_4}\ . \qquad (46)$$

To reduce (42) we will need the commutator

$$[B,\alpha_m^{\dagger(c)}] = -\sqrt{2}\sum_{m=1}^{\infty}\frac{1}{(m-1)!}[\partial_z^m \ln V_c(z)]_{z=0}\ . \qquad (47)$$

Partial derivatives of the projective transformation can easily be taken giving

$$\partial_z V_i(z=0) = \frac{a_1a_4-a_2a_3}{(a_3z+a_4)^2}|_{z=0} = \frac{(z_i-z_{i+1})(z_{i-1}-z_i)}{z_{i+1}-z_{i-1}}\ , \qquad (48)$$

or, more generally,

$$\partial_z^m V_i(z=0) = \frac{m!(-a_3)^{m-1}(a_1a_4-a_2a_3)}{(a_3z+a_4)^{m+1}}|_{z=0} = (-)^{m-1}m!\frac{(z_i-z_{i+1})^m(z_{i-1}-z_i)}{(z_{i+1}-z_{i-1})}\ . \qquad (49)$$

The single-loop three-point diagram is constructed by sewing together two legs of a five-point diagram, and then fixing three of the projective coordinates. For that case, following Di Vecchi *et al.* [24] we sew together legs 3 and 4 and then choose $z_3 = k$, $z_4 = \infty$, and $z_5 = 1$. In the present case, we will associate the coordinate $z_5$ with the connecting leg coordinate $z_c$. This gives $\partial_z V_c(z=0) = z_1 - 1$, along with $\partial_z^m V_c(z=0) = 0$ for $m \geq 2$. Thus, the commutator (47) becomes

$$[B,\alpha_m^{\dagger(c)}] = -\sqrt{2}\sum_{m=1}^{\infty}\frac{(-)^{m+1}[V_c'(z)]^m}{V_c(z)^m}|_{z=0} = \sqrt{2}\sum_{m=1}^{\infty}(1-z_1)^m\ . \qquad (50)$$

Next, the coefficient $C$ in (40) is given by

$$C = \sum_{i=1}^{3}\sum_{m=0}^{\infty} \alpha_0^{(i)} \cdot \alpha_m^{(i)} \frac{1}{m!}\partial_z^m \ln[V_i'(z)]_{z=0} + 2 \sum_{\substack{i,\,j\,=\,1 \\ i<j}}^{3} \sum_{n,m=0}^{\infty} \frac{\alpha_n^{(i)}}{n!} \cdot \frac{\alpha_m^{(j)}}{m!} \partial_y^n \partial_z^m \ln[V_i(y) - V_j(z)]_{y=z=0}$$

$$+ \sum_{i,j=1}^{3} \sum_{n,m=0}^{\infty} \frac{\alpha_n^{(i)}}{n!} \cdot \frac{\alpha_m^{(j)}}{m!} \partial_y^n \partial_z^m \ln \frac{E(V_i(y), V_j(z))}{V_i(y) - V_j(z)} |_{y=z=0} \ , \tag{51}$$

where the prime form is defined by

$$E(z,w) = (z-w) \prod_{\alpha}{}' \frac{z - T_\alpha(w)}{z - T_\alpha(z)} \frac{w - T_\alpha(z)}{w - T_\alpha(w)} \ , \tag{52}$$

and the prime indicates that the identity is not included. For a single loop the prime form reduces to

$$E(z,w) = (z-w) \prod_{n=1}^{\infty}{}' \frac{z - k^n w}{z - k^n z} \frac{w - k^n z}{w - k^n w} \ . \tag{53}$$

Below, we will also need the commutator

$$\langle 0|[C, \alpha_m^{\dagger(c)}]|0, p_i\rangle = \sum_{m=1}^{\infty} \frac{p}{(m-1)!} \partial_z^m \ln[V_c'(z)]_{z=0} + 2 \sum_{i \neq c} \sum_{m=1}^{\infty} \frac{p_i}{(m-1)!} \partial_z^m \ln[z_i - V_c(z)]_{z=0}$$

$$+2 \sum_{i} \sum_{m=1}^{\infty} \frac{p_i}{(m-1)!} \partial_z^m \ln \prod_{n=1}^{\infty} \frac{z_i - k^n V_c(z)}{z_i - k^n z_i} \frac{V_c(z) - k^n z_i}{V_c(z) - k^n V_c(z)} |_{z=0} \ , \tag{54}$$

where $p_c = p$. Because of momentum conservation, we can neglect the second denominator in the last term. Further, in the high-energy limit $s \to \infty$, we have $p_1 \cdot p_3 \to s/2$, $p_1 \cdot p_4 \to -s/2$, $p_2 \cdot p_3 \to -s/2$, and $p_2 \cdot p_4 \to s/2$. These imply

$$p \cdot p_i = (p_1 + p_2) \cdot p_i \to 0 \ . \tag{55}$$

Consequently, some terms in (54) do not survive the high-energy limit in (42). This permits us to drop the entire first term and the $i = c$ term in the last sum. Rearrangement then yields

$$\langle 0|[C, \alpha_m^{\dagger(c)}]|0, p_i\rangle = 2 \sum_{i \neq c} \sum_{m=1}^{\infty} \frac{p_i}{(m-1)!} \partial_z^m \left( \ln \prod_{n=0}^{\infty} [z_i - k^n V_c(z)] \prod_{r=1}^{\infty} [V_c(z) - k^r z_i] \right)_{z=0} \ . \tag{56}$$

Evaluating the derivatives gives

$$\langle 0|[C, \alpha_m^{\dagger(c)}]|0, p_i\rangle = 2 \sum_{i \neq c} p_i \left( \sum_{\substack{m\,=\,1 \\ n\,=\,0}}^{\infty} \frac{-k^{mn} [V_c'(z)]^m}{[z_i - k^n V_c(z)]^m} + \sum_{m,n=1}^{\infty} \frac{(-)^{m+1} [V_c'(z)]^m}{[V_c(z) - k^n z_i]^m} \right)_{z=0} \ , \tag{57}$$

which simplifies to

$$\langle 0|[C, \alpha_m^{\dagger(c)}]|0, p_i\rangle = -2 \sum_{i \neq c} p_i \left( \sum_{\substack{m\,=\,1 \\ n\,=\,0}}^{\infty} \frac{k^{mn} (1 - z_1)^m}{(k^n - z_i)^m} + \sum_{m,n=1}^{\infty} \frac{(1 - z_1)^m}{(1 - k^n z_i)^m} \right) \ . \tag{58}$$

Finally, we need the single-loop result

$$\exp\left[ -\frac{1}{2} \frac{B^2}{\ln k_1} + C \right] |0, p_1, p_2\rangle = \psi_{12}^{2p_1 \cdot p_2} |0, p_1, p_2\rangle \ , \tag{59}$$

where $\psi$ arises in planar loop amplitudes and can be expressed in terms of the Jacobi $\theta$ function. Substituting (50) and (58) into (42) then gives

$$A_{(4;2)} \simeq \int_0^1 dz\, z^{-1-\alpha(t)} \int d\mu \int_0^1 \prod_{i=1}^{4} dz_i \psi_{12}^{2p_1\cdot p_2} \psi_{34}^{2p_3\cdot p_4} \exp\Bigg\{ 2\sum_{m=1}^{\infty} \frac{z^m (1-z_1)^m (1-z_3)^m}{m} \Bigg[ \sum_{i,j} \frac{p_i\cdot p_j \ln z_i \ln z_j}{\ln k_1 \ln k_2}$$
$$- \sum_i \sum_{j\neq c} p_i\cdot p_j \frac{\ln z_i}{\ln k_1} \left( \sum_{n=0}^{\infty} \frac{k_2^{mn}}{(k_2^n - z_j)^m} + \sum_{n=1}^{\infty} \frac{1}{(1-k_2^n z_j)^m} \right)$$
$$- \sum_{i\neq c} \sum_j p_i\cdot p_j \frac{\ln z_j}{\ln k_2} \left( \sum_{n=0}^{\infty} \frac{k_1^{mn}}{(k_1^n - z_i)^m} + \sum_{n=1}^{\infty} \frac{1}{(1-k_1^n z_i)^m} \right)$$
$$+ \sum_{i,j\neq c} p_i\cdot p_j \left( \sum_{n=0}^{\infty} \frac{k_1^{mn}}{(k_1^n - z_i)^m} + \sum_{n=1}^{\infty} \frac{1}{(1-k_1^n z_i)^m} \right)$$
$$\times \left( \sum_{r=0}^{\infty} \frac{k_2^{mr}}{(k_2^r - z_j)^m} + \sum_{r=1}^{\infty} \frac{1}{(1-k_2^r z_j)^m} \right) \Bigg] \Bigg\} , \tag{60}$$

where $i$ and $j$ correspond to the different loops, and we have dropped a momentum-independent factor, which can be ignored in the high-energy limit. Replacing the momentum scalar products by their high-energy limits allows us to factorize the argument of the exponential to get

$$A_{(4;2)} \simeq \int_0^1 dz\, z^{-1-\alpha(t)} \int d\mu \int_0^1 \prod_{i=1}^{4} dz_i (\psi_{12}\psi_{34})^{-1-\alpha(t)}$$
$$\times \exp\left( s \sum_{m=1}^{\infty} \frac{z^m (1-z_1)^m (1-z_3)^m}{m} g_m(z_1,z_2,k_1) g_m(z_3,z_4,k_2) \right) , \tag{61}$$

where we have defined

$$g_m(x,y,k) = \frac{\ln x}{\ln k} - \sum_{n=0}^{\infty} \frac{k^{mn}}{(k^n - x)^m} - \sum_{n=1}^{\infty} \frac{1}{(1-k^n x)^m} - \langle x \leftrightarrow y \rangle . \tag{62}$$

The function $g_m(x,y,k)$ is for orientable planar loops and is essentially the $m$th derivative of $\ln\psi$. Thus, we can immediately write down the expression in the nonorientable case:

$$g_m^{\rm no}(x,y,k) = \frac{\ln x}{\ln k} - \sum_{n=0}^{\infty} \frac{(-k)^{mn}}{[(-k)^n - x]^m} - \sum_{n=1}^{\infty} \frac{1}{[1-(-k)^n x]^m} - \langle x \leftrightarrow y \rangle , \tag{63}$$

and for the nonplanar case:

$$g_m^{\rm np}(x,y,k) = \frac{\ln x}{\ln k} - \sum_{n=0}^{\infty} \frac{(-)^m k^{mn}}{(-k^n - x)^m} - \sum_{n=1}^{\infty} \frac{1}{(1+k^n x)^m} - \langle x \leftrightarrow y \rangle . \tag{64}$$

Now, we search for critical points, which do not reside on the boundary of the integration region. Unfortunately, due to its complicated form, one must numerically search for zeros in $g_m(x,y,k)$. It is found that $g_m(x,y,k)$, for all $m$, does indeed possess zeros that are exclusively within the integration range. These zeros generate the critical-point curve $x = P(y,k)$, for some function $P(y,k)$ that satisfies $g_m(P(y,k),y,k) = 0$. In addition, numerical analysis indicates that both nonorientable and nonplanar cases also possess critical-point curves. In all these cases the zeros do not seem to be confined to any particular region of integration space. This case differs from the tree calculation in two respects. First, to factorize Eq. (60) it was not necessary to impose a dimensionality constraint. Clearly, this is due to the fact that there are only four interacting particles and not because of the loops. Second, unlike the tree amplitudes, the presence of twists is not significant. In the former case, the twists were necessary to change the sign of some of the energies to place critical points inside the integration region. In the loop amplitudes, the signs change because of the periodicity of the Jacobi $\theta$ function.

Continuing with the calculation, in the limit $s \to i\infty$ (61) becomes

$$A_{(4;2)} \sim \int_0^1 dz\, z^{-1-\alpha(t)} \int d\mu \int_0^1 \prod_{i=1}^{4} dz_i (\psi_{12}\psi_{34})^{-1-\alpha(t)} e^{sz^2 h_2} \exp[sz(1-z_1)(1-z_3) g_1(z_1,z_2,k_1) g_1(z_3,z_4,k_2)] , \tag{65}$$

where

$$h_2 = \tfrac{1}{2}(1-z_1)^2 (1-z_3)^2 g_2(z_1,z_2,k_1) g_2(z_3,z_4,k_2) . \tag{66}$$

We will evaluate about the critical curve

$$|z_1 - P(z_2,k_1)| \le \epsilon \ , \quad |z_3 - P(z_4,k_2)| \le \epsilon \ . \tag{67}$$

Expanding the $g_1$'s about this curve, and then shifting $z_1$ and $z_3$, gives

$$A_{(4;2)} \sim \int_0^1 dz\, z^{-1-\alpha(t)} \int d\mu \int_0^1 dz_2 dz_4 (\psi_{12}\psi_{34})^{-1-\alpha(t)} e^{sz^2h_2} \int_{-\epsilon}^{\epsilon} dz_1 dz_3 \, \exp[szz_1z_3h_1] \ , \tag{68}$$

where

$$h_1 = [1-P(z_2,k_1)]^2[1-P(z_4,k_2)]^2 g_1'(z_1 = P(z_2,k_1), z_2, k_1) g_1'(z_3 = P(z_4,k_2), z_4, k_2) \ , \tag{69}$$

and $h_2$, $\psi_{12}$, and $\psi_{34}$ are now evaluated on the critical curve. The integration of $z_1$ and $z_3$ proceeds as before, giving

$$A_{(4;2)} \sim 2i\pi s^{-1} \int_0^1 dz\, z^{-2-\alpha(t)} \int d\mu \int_0^1 dz_2 dz_4 (\psi_{12}\psi_{34})^{-1-\alpha(t)} h_1^{-1} e^{sz^2h_2} \ . \tag{70}$$

Similarly, the $z$ integration is also easily done giving

$$A_{(4;2)} \sim -i\pi e^{-i\pi\alpha_2(t)} s^{\alpha_2(t)} \Gamma[-\alpha_2(t)-1] \int d\mu \int_0^1 dz_2 dz_4 (\psi_{12}\psi_{34})^{-1-\alpha(t)} h_1^{-1} h_2^{\alpha_2(t)+1} \ , \tag{71}$$

which exhibits the first sister trajectory $\alpha_2(t)$. Since the integrands involve derivatives of the Jacobi $\theta$ functions, we are unable to complete the calculation showing explicitly that the sister does not decouple. For the planar diagram, however, at $\alpha_2(t) = -1$ it can easily be shown that the signs of each of the integrand factors are the same over the entire integration region. On the other hand, to show that decoupling does not occur in the nonorientable and nonplanar cases is more difficult, although in the latter case there are indications that this does not happen [25].

The form of (61) suggests that higher-order sister trajectories may also exist. For example, the second sister $\alpha_3(t)$ is present if it can be shown that two of the $g$'s share the same critical point. Using

$$(1+x)^{-(r+1)} - (1+x)^{-r} = -xe^x \ , \tag{72}$$

it follows that

$$g_r(x,y,k) - g_{r+1}(x,y,k) = \sum_{n=1}^{\infty} (k^n x e^{-k^n x} - k^n y e^{-k^n y}) + \sum_{n=0}^{\infty} \left( \frac{x}{k^n} e^{-x/k^n} - \frac{y}{k^n} e^{-y/k^n} \right) \ . \tag{73}$$

Note that the right-hand side is independent of the index $r$. Thus, for any given critical point either one $g_r$ vanishes, resulting in a single sister, or they all vanish simultaneously giving the full sister spectrum. In the latter case, (61) reduces to the form

$$A_{(4;2)} \simeq \int_0^1 dz\, z^{-1-\alpha(t)} \int d\mu \int_0^1 dz_2 dz_4 (\psi_{12}\psi_{34})^{-1-\alpha(t)} \int_{-\epsilon}^{\epsilon} dz_1 dz_3 \, \exp\left( sz_1z_3 \sum_{m=1}^{\infty} z^m e_m \right) \ . \tag{74}$$

Integrating over $z_1$ and $z_3$, we obtain

$$A_{(4;2)} \simeq i\pi s^{-1} \int_0^1 dz\, z^{-1-\alpha(t)} \int d\mu \int_0^1 dz_2 dz_4 (\psi_{12}\psi_{34})^{-1-\alpha(t)} \left( \sum_{m=1}^{\infty} z^m e_m \right)^{-1} \ . \tag{75}$$

The right factor gives a $z^{-1}$ in leading order. Consequently, the $z$ integral generates a leading pole at $\alpha(t) = -1$, whereas the second sister requires $\alpha(t) = -2$. We conclude, then, that only the first sister can appear in double-loop processes.

Presumably, the $\alpha_3(t)$ trajectory is present if there are at least two loops on both sides of the propagator. We suspect that, in this case, there would be a factorization of the form

$$G_m(x,y,k_1,k_2) = g_m(x,y,k_1) g_m(x,y,k_2) \tag{76}$$

where $k_1$ and $k_2$ correspond to same-side loops. In Fig. 6 we display two distinct possible multiple-loop topologies for producing the higher-order sisters. In both cases the central propagator may allow up to the $m$th sister if there are at least $m$ loops on either side. However, evaluating Fig. 6(a) is not practical, since the Schottky representa-

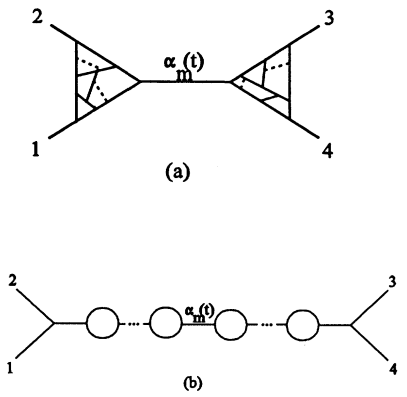


FIG. 6. Two distinct topologies for producing the $\alpha_m(t)$ sister in multiple-loop four-point scattering.

tion of the prime form (52) is generally intractable when two or more irreducible loops are present. On the other hand, since Fig. 6(b) completely factorizes the loops, the computation may not require many additional techniques beyond those presented in this section.

## IV. CONCLUDING REMARKS

In this paper we have tried to address the issue of locality in string theory. At a minimum, for locality to hold it is necessary that the upper bound constraint $|A(s,t)| \leq s^{|t|^{1/2}}$, shown by Martin to give the CM bound, be obeyed in the high-energy fixed $t$ limit. The key feature in our analysis is the sister trajectories, whose combined high-energy behavior may actually agree precisely with Martin's upper bound. We have made a first step in confirming this by showing that for four-point scattering the first sister appears at two-loop order. In general, to show that $N$-point scattering in string theory obeys the bound, the set of scattering amplitudes revealing the full spectrum of sisters trajectories must be evaluated. Each perturbative series must then be summed to obtain nonperturbative amplitudes, which are then to be checked against the bound.

An alternative is to show the CM bound directly using sister-dominated amplitudes. Unfortunately, at this time it is not clear how to take the fixed-angle limit with the high-energy approach employed in this paper. We may try to adopt the saddle-point method of Gross and Mende [8]. However, for the sister trajectories, the leading saddle-point expansion terms vanish in both the $s$ and $u$ channels. This leads to a predominantly fixed $t$ limit in fixed-angle scattering. As noted in Ref. [8], this is where the saddle points approach the boundary of integration space and their methods break down. As an aside, since the saddle points evaluated by Gross and Mende dominate those due to sister trajectories, their final amplitudes would actually exceed the lower CM bound if the sister generated amplitudes agree with the CM bound.

## ACKNOWLEDGMENTS

I would like to thank Charles Thorn for suggesting this problem, and for many useful discussions and comments. This work was supported in part by U.S. Department of Energy under Contract No. DE-FG05-86ER-40272, and a summer grant from the Institute for Fundamental Theory at the University of Florida.

[1] F. Cerulus and A. Martin, Phys. Lett. **8**, 80 (1964).
[2] G. Veneziano, Nuovo Cimento **57A**, 190 (1968).
[3] D. A. Eliezer and R. P. Woodard, Nucl. Phys. **B325**, 389 (1989).
[4] G. T. Horowitz, J. Morrow-Jones, S. P. Martin, and R. P. Woodard, Phys. Lett. **60B**, 261 (1988).
[5] D. J. Gross and P. F. Mende, Phys. Lett. B **197**, 129 (1987); Nucl Phys. **B303**, 407 (1988).
[6] C. B. Thorn (private communication).
[7] A. Martin, Nuovo Cimento **37**, 671 (1965).
[8] P. F. Mende and H. Ooguri, Nucl. Phys. **B339**, 641 (1990).
[9] P. Hoyer, N. A. Törnqvist, and B. R. Webber, Phys. Lett. **61B**, 191 (1976).
[10] P. Hoyer, Phys. Lett. **63B**, 50 (1976).
[11] W. J. Zakrzewski, Nucl. Phys. **B130**, 164 (1977).
[12] M. Sarbishaei and W. J. Zakrzewski, Nucl. Phys. **B132**, 268 (1977); **B132**, 294 (1977).
[13] C. Barratt, Nucl. Phys. **B120**, 147 (1977).
[14] M. Sarbishaei, W. J. Zakrzewski, and C. Barratt, Nucl. Phys. **B132**, 478 (1978).
[15] M. Quirós, Nucl. Phys. **B155**, 509 (1979).
[16] C. Barratt, Nucl. Phys. **B126**, 133 (1977).
[17] P. Hoyer and J. Kwiecinski, Nucl. Phys. **145**, 409 (1970).
[18] M. Quirós, Nucl. Phys. **B160**, 269 (1979).
[19] S. L. Carbon and C. B. Thorn, Phys. Rev. D **49**, R6264 (1994).
[20] P. Hoyer, N. A. Törnqvist, and B. R. Webber, Nucl. Phys. **B115**, 429 (1976).
[21] V. Alessandrini, D. Amati, and B. Morel, Nuovo Cimento A **7**, 797 (1972).
[22] Chan Hong-Mo, P. Hoyer, and P. V. Ruuskanen, Nucl. Phys. **B38**, 125 (1974).
[23] P. Di Vecchia, F. Pezzella, M. Frau, K. Hornfeck, A. Lerda, and S. Scuito, Nucl. Phys. **B322**, 317 (1989).
[24] P. Di Vecchia, M. Frau, A. Lerda, and S. Scuito, Nucl. Phys. **B298**, 526 (1988).
[25] S. L. Carbon (unpublished).